





# Decreased water exchange rate across blood–brain barrier in hereditary cerebral small vessel disease

Yingying Li,<sup>1,2,†</sup> Yunqing Ying,<sup>3,†</sup> Tingyan Yao,<sup>4,†</sup> Xuejia Jia,<sup>1,2</sup> Huilou Liang,<sup>5</sup> Weijun Tang,<sup>6</sup> Xiuqin Jia,<sup>1,2</sup> Haiqing Song,<sup>4</sup> Xingfeng Shao,<sup>7</sup> Danny J. J. Wang,<sup>7</sup> Chaodong Wang,<sup>4</sup>  Xin Cheng<sup>3</sup> and  Qi Yang<sup>1,2</sup>

<sup>†</sup>These authors contributed equally to this work.

Cerebral autosomal dominant arteriopathy with subcortical infarcts and leukoencephalopathy (CADASIL) and heterozygous *HTRA1* mutation-related cerebral small vessel disease (CSVD) are the two types of dominant hereditary CSVD. Blood–brain barrier (BBB) failure has been hypothesized in the pathophysiology of CSVD. However, it is unclear whether there is BBB damage in the two types of hereditary CSVD, especially in heterozygous *HTRA1* mutation-related CSVD.

In this study, a case-control design was used with two disease groups including CADASIL ( $n=24$ ), heterozygous *HTRA1* mutation-related CSVD ( $n=9$ ) and healthy controls ( $n=24$ ). All participants underwent clinical cognitive assessments and brain MRI. Diffusion-prepared pseudo-continuous arterial spin labelling was used to estimate the water exchange rate across the BBB ( $k_w$ ). Correlation and multiple linear regression analyses were used to examine the association between  $k_w$  and disease burden and neuropsychological performance, respectively.

Compared with the healthy controls,  $k_w$  in the whole brain and multiple brain regions was decreased in both CADASIL and heterozygous *HTRA1* mutation-related CSVD patients (Bonferroni-corrected  $P < 0.007$ ). In the CADASIL group, decreased  $k_w$  in the whole brain ( $\beta = -0.634$ ,  $P = 0.001$ ), normal-appearing white matter ( $\beta = -0.599$ ,  $P = 0.002$ ) and temporal lobe ( $\beta = -0.654$ ,  $P = 0.001$ ) was significantly associated with higher CSVD score after adjusting for age and sex. Reduced  $k_w$  in the whole brain was significantly associated with poorer neuropsychological performance after adjusting for age, sex and education in both CADASIL and heterozygous *HTRA1* mutation-related CSVD groups ( $\beta = 0.458$ ,  $P = 0.001$ ;  $\beta = 0.884$ ,  $P = 0.008$ ).

This study showed that there was decreased water exchange rate across the BBB in both CADASIL and heterozygous *HTRA1* mutation-related CSVD patients, suggesting a common pathophysiological mechanism underlying the two types of hereditary CSVD. These results highlight the potential use of  $k_w$  for monitoring the course of CADASIL and heterozygous *HTRA1* mutation-related CSVD, a possibility which should be tested in future research.

- 1 Department of Radiology, Beijing Chaoyang Hospital, Capital Medical University, Beijing 100020, China
- 2 Key Lab of Medical Engineering for Cardiovascular Disease, Ministry of Education, Beijing 100020, China
- 3 Department of Neurology, National Center for Neurological Disorders, National Clinical Research Centre for Aging and Medicine, Huashan Hospital, Fudan University, Shanghai 200040, China
- 4 Department of Neurology, Xuanwu Hospital, Capital Medical University, National Clinical Research Center for Geriatric Disorders, Beijing 100053, China
- 5 State Key Laboratory of Brain and Cognitive Science, Beijing MRI Center for Brain Research, Institute of Biophysics, Chinese Academy of Sciences, Beijing 100101, China

Received August 09, 2022. Revised December 07, 2022. Accepted December 18, 2022. Advance access publication January 10, 2023

© The Author(s) 2023. Published by Oxford University Press on behalf of the Guarantors of Brain.

This is an Open Access article distributed under the terms of the Creative Commons Attribution-NonCommercial License (<https://creativecommons.org/licenses/by-nc/4.0/>), which permits non-commercial re-use, distribution, and reproduction in any medium, provided the original work is properly cited. For commercial re-use, please contact [journals.permissions@oup.com](mailto:journals.permissions@oup.com)

6 Department of Radiology, Huashan Hospital, Fudan University, Shanghai 200040, China

7 Laboratory of FMRI Technology (LOFT), USC Mark & Mary Stevens Neuroimaging and Informatics Institute, Keck School of Medicine, University of Southern California, Los Angeles, CA 90033, USA

Correspondence to: Chaodong Wang, MD, PhD  
Department of Neurology  
Xuanwu Hospital, Capital Medical University  
No. 45 Changchun Road, Xicheng District, Beijing 100053, China  
E-mail: cdongwang01@126.com

Correspondence may also be addressed to: Xin Cheng, MD, PhD  
Department of Neurology  
Huashan Hospital, Fudan University  
No. 12 Wulumuqizhong Road, Jingan District, Shanghai 200040, China  
E-mail: chengxin@fudan.edu.cn

Qi Yang, MD, PhD  
Department of Radiology  
Beijing Chaoyang Hospital  
Capital Medical University  
No. 8 Gongti South Road, Chaoyang District, Beijing 100020, China  
E-mail: yangyangqiqi@gmail.com

**Keywords:** CADASIL; heterozygous *HTRA1* mutation-related CSVD; blood–brain barrier; magnetic resonance imaging; water exchange rate ( $k_w$ )

## Introduction

Blood–brain barrier (BBB) failure has been hypothesized in the pathophysiology of cerebral small vessel disease (CSVD).<sup>1,2</sup> Dynamic contrast-enhanced (DCE) MRI has been the most widely applied method for evaluating BBB damage in clinical research. It tracks paracellular leakage of gadolinium contrast agents as it passes between the blood and brain ( $K_{trans}$ ).<sup>1,3</sup> Cerebral autosomal dominant arteriopathy with subcortical infarcts and leukoencephalopathy (CADASIL) is an autosomal dominant CSVD caused by *NOTCH3* gene mutations.<sup>4</sup> Several studies have applied DCE-MRI to assess BBB damage in CADASIL.<sup>5,6</sup>

However, there are inconsistencies in existing research on BBB damage in CADASIL. One study showed that  $K_{trans}$  in patients with CADASIL was increased and related to iron deposition in specific brain regions,<sup>5</sup> while another study reported that  $K_{trans}$  in patients with CADASIL did not change, and it was speculated that increased BBB permeability played a less important role in the disease process of CADASIL.<sup>6</sup> Notably, BBB damage not only includes structural damage, but also functional impairment of the BBB.<sup>7</sup> As gadolinium contrast is an exogenous tracer with a relatively large molecular weight (550 Da), DCE-MRI may be less suited to assess more subtle forms of BBB dysfunction associated with alterations in transport systems.<sup>1,8,9</sup>

Diffusion-prepared pseudo-continuous arterial spin labelling imaging (DP-pCASL) is a new MRI technique enabling the quantification of water exchange rate ( $k_w$ ) across the BBB.<sup>10–12</sup> Water is an endogenous tracer with a small molecular weight (~18 Da). Therefore, the evaluation of BBB water exchange may achieve a more sensitive assessment of BBB damage at the early stage of disease progression.<sup>13–15</sup> In addition, water crosses the BBB mainly through simple diffusion, aquaporin-4 (AQP4) and some cotransport proteins located in the endothelium membrane (such as  $Na^+/K^+/Cl^-$  co-transporters, glucose transporters and monocarboxylate transporters).<sup>8,16–18</sup> Thus, DP-pCASL is also suitable to assess

BBB dysfunction associated with alterations in transport systems compared with DCE-MRI.<sup>13,15</sup> Moreover, DP-pCASL allows for the computation of metrics of cerebral perfusion such as cerebral blood flow (CBF) and arterial transit time (ATT).<sup>14</sup> Evaluating  $k_w$  in conjunction with CBF and ATT based on DP-pCASL may provide a sensitive and comprehensive approach to determine and quantify BBB damage in CADASIL.

In addition to CADASIL, heterozygous *HTRA1* mutation is the second most common cause of autosomal dominant CSVD.<sup>19,20</sup> A growing number of heterozygous *HTRA1* mutation-related CSVD cases has been detected in clinical practice.<sup>21</sup> Similar to other types of CSVD, the typical imaging characteristics of heterozygous *HTRA1* mutation-related CSVD are white matter hyperintensity (WMH), lacunes, enlarged perivascular spaces (ePVS) and microbleeds.<sup>19,21</sup> However, it is unclear whether there is BBB damage in heterozygous *HTRA1* mutation-related CSVD, moreover, whether heterozygous *HTRA1* mutation-related CSVD involves BBB damage, if there is a correlation between BBB damage and typical imaging characteristics and whether the severity of BBB damage is comparable with that of CADASIL.

Here, we report the first measurement of the quantitative  $k_w$  across the BBB in patients with CADASIL and heterozygous *HTRA1* mutation-related CSVD. We hypothesized that both CADASIL and heterozygous *HTRA1* mutation-related CSVD exhibit decreased BBB water exchange and the extent of BBB  $k_w$  reduction matches the disease burden of CSVD, respectively. This study aimed to unveil altered BBB water exchange and highlight the potential of this imaging technique for monitoring disease activity in patients with CADASIL and heterozygous *HTRA1* mutation-related CSVD.

## Materials and methods

### Participants and neuropsychological assessments

In this study, we enrolled 24 CADASIL and 9 heterozygous *HTRA1* mutation-related CSVD patients and 24 age- and sex-matched

healthy controls. The inclusion criterion for patients with CADASIL was a confirmed genetic diagnosis of typical mutation of the NOTCH3 gene. The inclusion criterion for patients with heterozygous HTRA1 mutation-related CSVD was a confirmed genetic diagnosis of heterozygous HTRA1 mutation (Supplementary Table 1). Participants with any history of head injury, alcoholism, drug abuse or severe psychiatric illness that might impair cognition were excluded.

We collected the following information at the time of inclusion from each participant: age, sex, years of education and vascular risk factors [transient ischaemic attack (TIA) or stroke, smoking, alcohol consumption, hypertension, diabetes mellitus, dyslipidaemia]. Cognitive function was globally assessed using the Mini-Mental State Examination (MMSE). Executive function was measured using the Trail-Making Test (TMT) Parts A and B, the Digit Span Task (Backward) and the Stroop Colour and Word Test.<sup>5</sup> Memory was measured using the Auditory Verbal Learning Test (AVLT). Visuospatial ability was measured using the Rey–Osterrieth complex figure. Language was measured using the verbal fluency test. Depressive symptoms were assessed through the Hamilton Depression Scale (HAM-D).<sup>22</sup> This study was approved by the Institutional Review Board and Ethics Committee at Beijing Chaoyang Hospital and Huashan Hospital. Written informed consent was obtained from each participant.

### MRI data acquisition

Participants were scanned on a Siemens 3 T Prisma MRI system (Siemens), using a 64-channel head coil. The MRI protocol included T<sub>1</sub>-weighted magnetization-prepared rapid acquisition gradient echo (MP-RAGE) images [resolution = 1 × 1 × 1 mm<sup>3</sup>, inversion time/echo time (TE)/repetition time (TR) = 900/2.98/2300 ms]; T<sub>2</sub>-weighted images [TE/TR = 94/4000 ms, flip angle = 150°, field of view (FOV) = 230 mm × 230 mm, matrix size = 320 × 230]; T<sub>2</sub>-weighted fluid attenuated inversion recovery (FLAIR) images (resolution = 1 × 1 × 1 mm<sup>3</sup>, inversion time/TE/TR = 1800/388/5000 ms); and susceptibility-weighted images (TE/TR = 20/28 ms, flip angle = 15°, FOV = 220 mm × 220 mm, matrix size = 256 × 220). DP-pCASL data were obtained using a 3D gradient-and-spin-echo DP-pCASL sequence [resolution = 3.5 × 3.5 × 8 mm<sup>3</sup>, TE/TR = 36.5/4000 ms, flip angle = 120°, FOV = 224 mm × 224 mm, matrix size = 64 × 64, 12 slices (10% oversampling), label/control duration = 1500 ms], centric ordering and optimized timing of background suppression for grey and white matter.<sup>13,23</sup>

### Cerebral small vessel disease imaging characteristics analysis

The typical imaging characteristics of CSVD (WMH, lacunes, ePVS and microbleeds) were defined as previously described.<sup>24</sup> The volume of WMH was automatically measured on FLAIR images using the lesion segmentation tool toolbox. To account for variation in brain volume, we normalized WMH to whole brain volume. The total CSVD score<sup>25</sup> was used to evaluate the disease burden of CADASIL and heterozygous HTRA1 mutation-related CSVD. The MRI lesions were assessed by two radiologists with more than 5 years of experience in neuroradiology.

### Diffusion-prepared pseudo-continuous arterial spin labelling imaging analyses

Post-processing of DP-pCASL data was performed offline using LOFT BBB Toolbox (<http://www.loft-lab.org/index-5.html>). Control/

label images were corrected for rigid head motion and subtracted to obtain perfusion images. The tissue and capillary compartments of the ASL signal were separated by a small diffusion gradient of 50 s/mm<sup>2</sup>. Using the flow encoding arterial spin tagging scan, ATT was calculated from scans acquired at diffusion weighting (b value) of 0 and 14 s/mm<sup>2</sup> and post-labelling delay (PLD) = 900 ms. The  $k_w$  map was calculated by a total-generalized-variation (TGV) regularized single-pass approximation (SPA) model using the tissue (or capillary) fraction of the ASL signal at b = 0 and 50 s/mm<sup>2</sup> and PLD = 1800 ms, incorporating ATT, T<sub>1</sub> of arterial blood (1.66 s) and brain tissue as inputs for the algorithm. CBF was quantified from perfusion signals acquired at PLD = 1800 ms without diffusion preparation as described in detail elsewhere.<sup>12,14</sup> A voxel-wise tissue T<sub>1</sub> map was fitted from background suppressed control images acquired at two PLDs.<sup>26</sup>

The  $k_w$ , CBF and ATT maps, along with the M0 (T<sub>2</sub>-weighted structural image in the same space), were co-registered to T<sub>1</sub>-weighted images and normalized to Montreal Neurological Institute (MNI) space for regional analysis. Average values were measured in the whole brain and regions of interests of relevance to CSVD and vascular cognitive impairment: normal-appearing white matter (NAWM), frontal lobe, temporal lobe, parietal lobe, caudate nucleus and putamen.<sup>14,27–30</sup> White matter mask was segmented by SPM12 from T<sub>1</sub>-weighted MP-RAGE images. WMH was excluded from white matter to form the NAWM mask. Other regions of interest were selected from the Anatomical Labeling Template in SPM12, using participants' T<sub>1</sub>-weighted images, as described previously.<sup>31</sup>

### Statistical analysis

The Shapiro–Wilk test was used to evaluate the normality of the data. Continuous variables are presented as the mean ± SD or median with interquartile range (IQR), and categorical variables are presented as proportions. A Student's t-test or Mann–Whitney U-test was used to analyse continuous data of the two groups. One-way analysis of variance or the Kruskal–Wallis test with Bonferroni-correction was used to analyse continuous data of the three groups. The chi-square test was used for categorical data. To compare  $k_w$ , CBF and ATT among the three groups, Bonferroni correction was applied to correct for the number of regions of interest tested ( $P = 0.05/7 = 0.007$ ).

Correlation of  $k_w$  and CSVD burden was first analysed using Spearman rank correlation. If the results of univariate correlation analysis were statistically significant, multivariate linear regression (stepwise) was performed to correct for age and sex, and Bonferroni correction was used to correct the number of regions of interest tested. Correlation of  $k_w$  and neuropsychological performance was first analysed using univariate Pearson or Spearman rank correlation. If the results of the univariate correlation analysis were statistically significant, multivariate linear regression (stepwise) was performed to correct for age, sex and education level. The significance of these regression models underwent Bonferroni correction by the total number of comparisons [ $P = 0.05/(\text{number of regions of interest} \times \text{number of cognitive function domains})$ ]. Statistical analyses were performed using IBM SPSS 26.0 and GraphPad Prism 9.2.

### Data availability

The data that support the findings of this study are available from the corresponding author, upon reasonable request.

## Results

### Subject characteristics

Demographic data, vascular risk factors and imaging characteristics of the healthy controls and patients with CADASIL and heterozygous *HTRA1* mutation-related CSVD are shown in Table 1. There were no significant differences in sex, age and years of education between the three groups, and there was no significant difference in the history of TIA/stroke and vascular risk factors between CADASIL and heterozygous *HTRA1* mutation-related CSVD group. WMH, lacunes, ePVS and microbleeds were detected in both CADASIL and heterozygous *HTRA1* mutation-related CSVD (Fig. 1).

All patients with CADASIL and healthy controls underwent all neuropsychological assessments. Due to coronavirus disease 2019 (COVID-19) and patients with heterozygous *HTRA1* mutation-related CSVD living in other cities, they did not have sufficient time to complete all cognitive assessments, so they only underwent MMSE and HAMD testing, and the assessment of other cognitive function domains were replaced by Montreal Cognitive Assessment (MoCA) subdomains.<sup>32</sup> There was significant difference in executive function and memory between the CADASIL and healthy control group, and there was significant difference in visuospatial/executive ability and attention score between the heterozygous *HTRA1* mutation-related CSVD and the healthy control group; the details are shown in Supplementary Table 2.

### Altered $k_w$ and cerebral perfusion in CADASIL and heterozygous *HTRA1* mutation-related cerebral small vessel disease groups

Compared with the healthy control group, the CADASIL group showed significantly decreased  $k_w$  in the whole brain, NAWM, frontal lobe, temporal lobe and putamen ( $P < 0.007$ ); the heterozygous *HTRA1* mutation-related CSVD group showed significantly decreased  $k_w$  in the whole brain, NAWM, frontal lobe, parietal lobe, temporal lobe and putamen ( $P < 0.007$ ). Compared with the CADASIL group, the heterozygous *HTRA1* mutation-related CSVD group showed significantly decreased  $k_w$  in whole the brain (Table 2, Fig. 2 and Supplementary Fig. 1).

Compared with the healthy control group, the CADASIL group and heterozygous *HTRA1* mutation-related CSVD group both showed significantly decreased CBF in the whole brain, NAWM, frontal lobe, parietal lobe and temporal lobe, and increased ATT in the temporal lobe ( $P < 0.007$ ). There was no significant difference in CBF and ATT between CADASIL and heterozygous *HTRA1* mutation-related CSVD group (Supplementary Tables 3 and 4 and Fig. 2).

### Relationships between $k_w$ and disease burden in CADASIL and heterozygous *HTRA1* mutation-related cerebral small vessel disease groups

In the CADASIL group, correlation analysis showed that decreased  $k_w$  in the whole brain, NAWM, temporal lobe and putamen was significantly associated with higher CSVD score (Fig. 3). These four brain regions were included in multiple linear regression analysis with age and sex as covariates, respectively, and the results showed that decreased  $k_w$  in the whole brain ( $\beta = -0.634$ ,  $P = 0.001$ ), NAWM ( $\beta = -0.599$ ,  $P = 0.002$ ) and temporal lobe ( $\beta = -0.654$ ,  $P = 0.001$ ) was significantly associated with higher CSVD score after adjusting for age and sex.

In the heterozygous *HTRA1* mutation-related CSVD group, correlation analysis showed decreased  $k_w$  in the temporal lobe was significantly associated with higher CSVD score (Fig. 3). This brain region was included in multiple linear regression analysis with age and sex as covariates, and the result showed that  $k_w$  in the temporal lobe was not significantly associated with CSVD score after adjusting for age and sex.

### Relationships between $k_w$ and neuropsychological performance in two types of hereditary cerebral small vessel disease

In the CADASIL group, correlation analysis showed that decreased  $k_w$  in the whole brain, NAWM, frontal lobe, temporal lobe and putamen was significantly associated with lower memory scores (AVLT immediate/long delayed recall score; Fig. 4). These five brain regions and two neuropsychological tests were included in multiple linear regression analysis with age, sex and education as covariates, respectively, and the results showed that decreased  $k_w$  in the whole brain ( $\beta = 0.458$ ,  $P = 0.001$ ), NAWM ( $\beta = 0.474$ ,  $P = 0.001$ ), frontal lobe ( $\beta = 0.401$ ,  $P = 0.004$ ) and putamen ( $\beta = 0.480$ ,  $P < 0.001$ ) was significantly associated with lower memory scores after adjusting for age, sex and education (Supplementary Table 5).

In the heterozygous *HTRA1* mutation-related CSVD group, correlation analysis showed that decreased  $k_w$  in the whole brain, NAWM, frontal lobe, parietal lobe and temporal lobe was significantly associated with lower attention score (Fig. 4). These five brain regions and one MoCA subdomain were included in multiple linear regression analysis with age, sex and education as covariates, respectively, and the result showed that decreased  $k_w$  in the whole brain ( $\beta = 0.884$ ,  $P = 0.008$ ) was significantly associated with lower attention scores after adjusting for age, sex and education (Supplementary Table 5).

## Discussion

Using an advanced MRI with DP-pCASL technique, we compared the water exchange rate across the BBB ( $k_w$ ) among CADASIL, heterozygous *HTRA1* mutation-related CSVD and healthy individuals and analysed the correlations with disease burden of CSVD and neuropsychological scores. These results revealed that there was decreased  $k_w$  in both CADASIL and heterozygous *HTRA1* mutation-related CSVD, and the reduced  $k_w$  was associated with higher disease burden and poorer neuropsychological performance.

The results of this study demonstrated that compared with healthy controls, both CADASIL and heterozygous *HTRA1* mutation-related CSVD showed reduced  $k_w$  within the whole brain, NAWM, frontal lobe, temporal lobe and putamen. Previous studies have shown that decreased  $k_w$  could reflect decreased localization or expression of AQP4.<sup>13,15</sup> Pathological study of CADASIL subjects showed that both chronic hypoperfusion of brain tissue<sup>33,34</sup> and NOTCH3 gene mutations<sup>35</sup> could lead to apoptosis of astrocytes and increased clasmotodendritic astrocytes with displaced AQP4, which ultimately leads to reduced AQP4 expression in the BBB.<sup>35</sup> The reduced  $k_w$  in CADASIL patients in the present study is consistent with the pathological findings in CADASIL. The reduced  $k_w$  in heterozygous *HTRA1* mutation-related CSVD patients suggests that there may be reduced AQP4 expression in the BBB in heterozygous *HTRA1* mutation-related CSVD.

AQP4 is not only a water channel, which also serves an important function in the brain's glymphatic system, a mechanism for the elimination of soluble material from the CNS.<sup>36,37</sup> In animal models



**Table 1** Demographic and vascular risk factors, and imaging characteristics for the healthy control group, CADASIL group and heterozygous *HTRA1* mutation-related CSVD group

	HC	CADASIL	HTRA1	P-value
Number	24	24	9	
Age, years	42.88 ± 12.34	44.17 ± 14.14	42.78 ± 15.14	0.936
Sex, male	6/24	9/24	6/9	0.087
Education	9.00 (11.00)	11.08 ± 4.60	12.00 (6.50)	0.590
Vascular risk factors				
TIA/stroke	0/24	8/24	6/9	<0.001 <sup>a,b</sup>
Smoking	2/24	4/20	6/9	0.002 <sup>b,c</sup>
Alcohol consumption	4/20	4/20	3/9	0.490
Hypertension	0/24	1/24	0/9	1.000
Diabetes mellitus	0/24	1/24	0/9	1.000
Dyslipidaemia	6/18	1/23	0/9	0.063
Imaging characteristics				
WMH volume	0.05 (0.19)	17.46 ± 12.05	15.45 ± 14.58	<0.001 <sup>a,b</sup>
Normalized WMH volume ratio	0.371 × 10 <sup>-4</sup> (0.00014)	0.012 ± 0.009	0.010 ± 0.010	<0.001 <sup>a,b</sup>
Lacunar infarcts	0/24	11/24	6/9	<0.001 <sup>a,b</sup>
Microbleeds	0/24	12/24	6/9	<0.001 <sup>a,b</sup>
ePVS	0/24	10/24	4/9	<0.001 <sup>a,b</sup>
CSVD score	–	2.00 (1.75)	3.50 (3.75)	–

Data are mean ± SD or median (IQR). HC = healthy controls.

<sup>a</sup>For the comparison between the CADASIL and HC (Bonferroni-corrected  $P < 0.05$ ).

<sup>b</sup>For the comparison between the HTRA1 and HC (Bonferroni-corrected  $P < 0.05$ ).

<sup>c</sup>For the comparison between the CADASIL and HTRA1 (Bonferroni-corrected  $P < 0.05$ ).

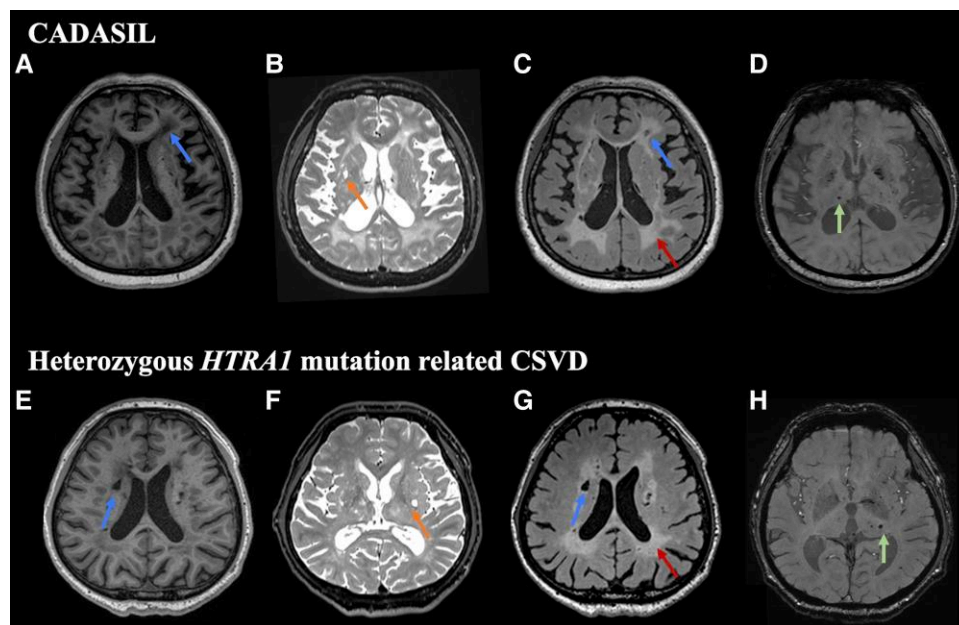


**Figure 1** Schematic representation of typical imaging characteristic of CADASIL and heterozygous *HTRA1* mutation-related CSVD patients. T<sub>1</sub>-weighted images (A and E), T<sub>2</sub>-weighted images (B and F) and FLAIR images (C and G) show diffuse white matter hyperintensities (red arrows), lacunes (blue arrows) and enlarged perivascular spaces (orange arrows), while gradient echo images (D and H) show microbleeds (green arrows) in both CADASIL (A–D; 51-year-old female) and heterozygous *HTRA1* mutation-related CSVD (E–H; 51-year-old male) patients.

with AQP4 deficiency, there is decreased  $k_w$ <sup>16</sup> and excessive A $\beta$  brain deposition.<sup>38</sup> In older adults, decreased  $k_w$  is associated with increased brain iron<sup>15</sup> and amyloid- $\beta$ .<sup>13</sup> In addition to AQP4, the cotransport proteins located in the endothelial membrane are also a way of water transport across the BBB.<sup>18</sup> Endothelial cell dysfunction may lead to decreased  $k_w$ . Furthermore, evidence suggests that endothelial cell dysfunction could lead to deficit in

local CBF regulation, which results in decreased CBF.<sup>39</sup> Based on this, reduced  $k_w$  in CADASIL and heterozygous *HTRA1* mutation-related CSVD suggests that there may be endothelial cell dysfunction or worsened BBB-related clearance function in both types of hereditary CSVD.

Heterozygous *HTRA1* mutation-related CSVD is a newly reported type of hereditary CSVD,<sup>19–21</sup> different from cerebral

Table 2 Comparison of  $k_w$  ( $\text{min}^{-1}$ ) between CADASIL, heterozygous HTRA1 mutation-related CSVD and healthy control groups

Brain regions	HC	CADASIL	HTRA1	P-value
Whole brain	133.19 ± 18.16	117.31 ± 23.70	95.13 ± 26.17	<0.001 <sup>a,b,c</sup>
NAWM	120.30 ± 16.94	102.96 ± 20.91	80.81 ± 25.98	<0.001 <sup>a,b</sup>
Frontal lobe	118.52 ± 14.05	95.50 ± 23.06	79.22 ± 22.98	<0.001 <sup>a,b</sup>
Parietal lobe	94.82 ± 18.98	83.64 ± 21.51	68.22 ± 19.39	0.006 <sup>b</sup>
Temporal lobe	112.36 ± 18.31	97.39 ± 25.36	81.45 ± 23.31	0.003 <sup>a,b</sup>
Caudate nucleus	114.72 ± 18.39	99.89 ± 25.83	91.02 ± 31.72	0.026
Putamen	132.18 ± 23.39	117.32 ± 22.33	102.66 ± 23.05	0.006 <sup>a,b</sup>

Data are mean ± SD or median (IQR). HC = healthy controls.

<sup>a</sup>For the comparison between the CADASIL and HC (Bonferroni-corrected  $P < 0.05$ ).

<sup>b</sup>For the comparison between the HTRA1 and HC (Bonferroni-corrected  $P < 0.05$ ).

<sup>c</sup>For the comparison between the CADASIL and HTRA1 (Bonferroni-corrected  $P < 0.05$ ).

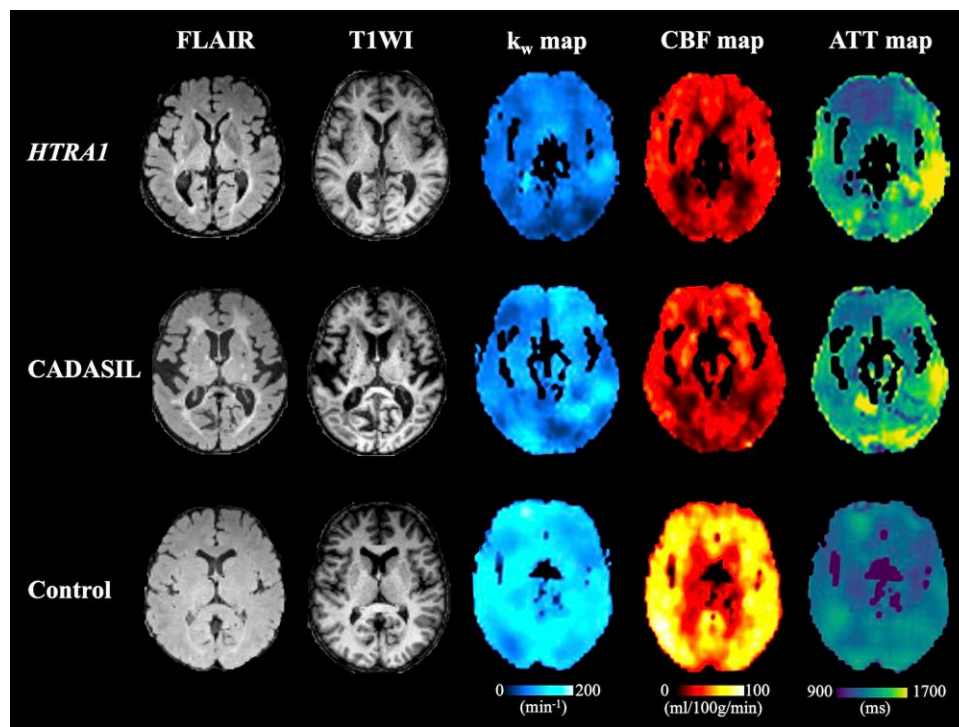


Figure 2 Decreased  $k_w$ , CBF and increased ATT in the heterozygous HTRA1 mutation-related CSVD and CADASIL patients compared with a healthy control. Example images from a representative patient with heterozygous HTRA1 mutation-related CSVD (51-year-old male; top row), a patient with CADASIL (51-year-old female; middle row) and a healthy control (50-year-old female; bottom row). In the patient with heterozygous HTRA1 mutation-related CSVD: average  $k_w = 82.8 \text{ min}^{-1}$ , average CBF = 28.3 ml/100 g/min, average ATT = 1357.5 ms; in the patient with CADASIL: average  $k_w = 103.5 \text{ min}^{-1}$ , average CBF = 28.6 ml/100 g/min, average ATT = 1365.6 ms; in the healthy control: average  $k_w = 126.8 \text{ min}^{-1}$ , average CBF = 52.4 ml/100 g/min, average ATT = 1223.4 ms.

autosomal recessive arteriopathy with subcortical infarcts and leukoencephalopathy (CARASIL), which is caused by biallelic mutations of the HTRA1.<sup>40</sup> Heterozygous HTRA1 mutation-related CSVD is dominant hereditary CSVD and has a higher incidence rate. Previous studies have suggested heterozygous mutations of HTRA1 to be the second most common cause of autosomal dominant SVD after CADASIL.<sup>19</sup> The results of this study showed that both types of autosomal dominant CSVD have BBB dysfunction, suggesting a common pathophysiological mechanism underlying the two types of hereditary CSVD. Furthermore, compared with the CADASIL group, the heterozygous HTRA1 mutation-related CSVD group showed reduced  $k_w$  within the whole brain. This finding suggests that the degree of BBB dysfunction of the two types of

hereditary CSVD may be inconsistent. In addition, ATT was prolonged in the temporal lobe in both hereditary CSVD, indicating the possible occurrence of small arteriolar stenosis. The temporal lobe is a brain region frequently involved in CADASIL.<sup>40</sup> This finding suggests that in heterozygous HTRA1 mutation-related CSVD, the temporal lobe may also be a brain region that is affected by small vessel pathology. Notably, the speculation regarding the pathological manifestation of heterozygous HTRA1 mutation-related CSVD in this study needs to be determined in future pathological studies.

Cerebral small vessel disease is one of the most important causes of dementia.<sup>22,29</sup> In the current study, executive function and memory decline occur in CADASIL patients; visuospatial/

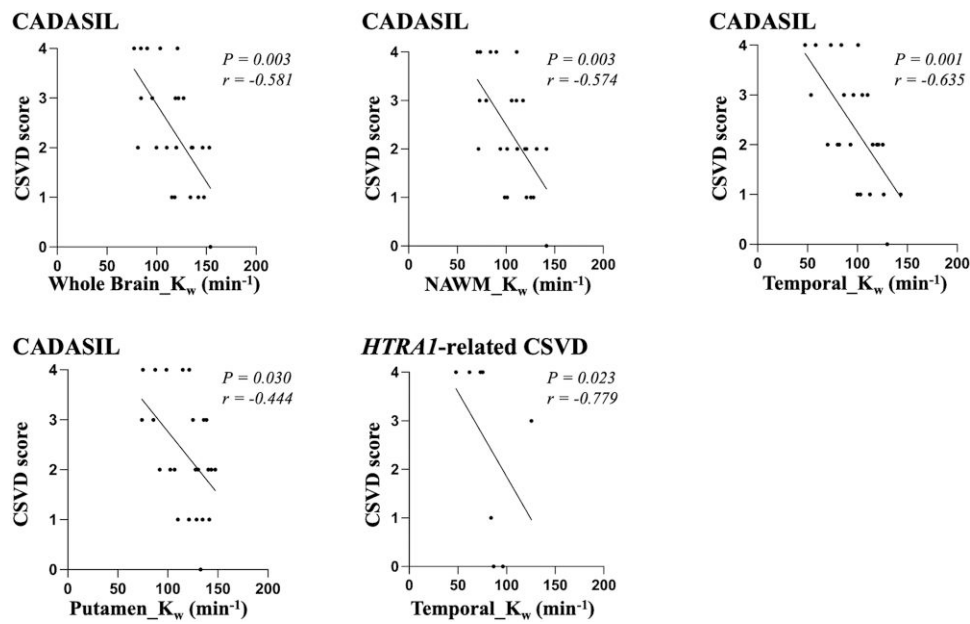


Figure 3 Correlations between  $k_w$  and CSVD score in CADASIL and heterozygous HTRA1 mutation-related CSVD groups.

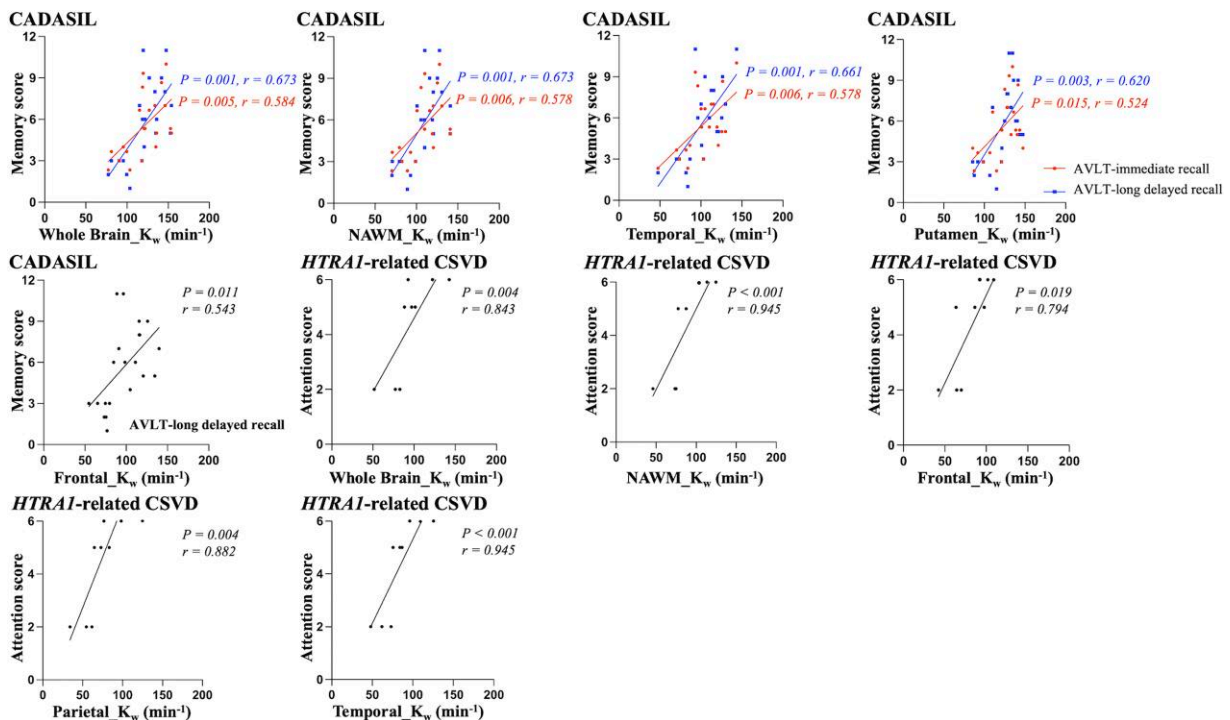


Figure 4 Correlations between  $k_w$  and neuropsychological performance in CADASIL group.

executive ability and attention decline occur in heterozygous HTRA1 mutation-related CSVD patients. Multiple linear regression analyses revealed that decreased  $k_w$  in the whole brain was significantly associated with poorer neuropsychological performance after adjusting for age, sex and education in both CADASIL and heterozygous HTRA1 mutation-related CSVD group. Moreover,

decreased  $k_w$  in the whole brain, NAWM and temporal lobe was also associated with the higher disease burden after adjusting for age and sex in the CADASIL group. As mentioned above, reduced  $k_w$  suggests that there may be BBB dysfunction associated with clearance, which may lead to the accumulation of blood-derived neurotoxic proteins in the CNS, resulting in neuronal injury,

disrupted structural and functional brain connectivity.<sup>7,41</sup> This result suggests that  $k_w$  has the potential for the evaluation of disease burden and cognitive decline in CADASIL and heterozygous *HTRA1* mutation-related CSVD.

This study has several limitations. First, given the rarity of heterozygous *HTRA1* mutation-related CSVD, the sample size of patients in this study is relatively small. Second, we only compared MMSE and HAMD between the three groups. Because other neuropsychological tests were different between CADASIL and heterozygous *HTRA1* mutation-related CSVD, they were compared separately with the control group. The statistical methods for this analysis may not be optimal and we were unable to assess differences in memory, language and executive function between CADASIL and heterozygous *HTRA1* mutation-related CSVD. Third, the specific direction of  $k_w$  alterations (lower  $k_w$  versus higher  $k_w$ ) in various ethnic groups requires further research. The present study and another study<sup>15</sup> showed that reduced  $k_w$  was associated with poorer neuropsychological performance in Asian populations with a range of CSVD stages and cognitive impairments, while a previous study showed that increased  $k_w$  was associated with increased vascular risk factors in a Latino cohort with generally mild CSVD.<sup>12</sup> Fourth, this study can only indicate that BBB dysfunction is the predominant form of BBB damage in both hereditary CSVD; future studies combining DCE-MRI will help to clarify the extent of BBB structural damage. In addition, the spatial resolution and signal-to-noise ratio of  $k_w$  and CBF maps are relatively low compared to standard ASL images due to the use of diffusion preparation and TGV regularized modelling. Moreover, it should be recognized that this is a cross-sectional study limited to a description of associations. Whether dysfunction of the BBB is responsible for disease progression of CADASIL and heterozygous *HTRA1* mutation-related CSVD remains unclear. Future work investigating  $k_w$  in longitudinal data sets is essential for answering these critical questions and driving the field forward.

In conclusion, this study revealed decrease of water exchange rate across the BBB in patients with CADASIL and heterozygous *HTRA1* mutation-related CSVD, suggesting a common pathophysiological mechanism underlying the two hereditary CSVD. These results highlight the potential use of  $k_w$  for monitoring the course of CADASIL and heterozygous *HTRA1* mutation-related CSVD, a possibility which should be tested in future research.

## Funding

This work was supported by grants from the National Natural Science Foundation of China (81961128030, 82025018, 81971123, 92249301), US National Institutes of Health grant R01NS114382, Capital's Funds for Health Improvement and Research (CFH-2022-1-2031), Beijing Hospitals Authority's Ascent Plan (DFL20220303) and Shanghai Municipal Committee of Science and Technology (20Z11900802).

## Competing interests

The authors report no competing interests.

## Supplementary material

Supplementary material is available at *Brain* online.

## References

- Thrippleton MJ, Backes WH, Sourbron S, et al. Quantifying blood–brain barrier leakage in small vessel disease: Review and consensus recommendations. *Alzheimers Dement*. 2019;15: 840–858.
- Blair GW, Hernandez MV, Thrippleton MJ, Doubal FN, Wardlaw JM. Advanced neuroimaging of cerebral small vessel disease. *Curr Treat Options Cardiovasc Med*. 2017;19:56.
- Rebeles F, Fink J, Anzai Y, Maravilla KR. Blood–brain barrier imaging and therapeutic potentials. *Top Magn Reson Imaging*. 2006; 17:107–116.
- Joutel A, Corpechot C, Ducros A, et al. Notch3 mutations in CADASIL, a hereditary adult-onset condition causing stroke and dementia. *Nature*. 1996;383:707–710.
- Uchida Y, Kan H, Sakurai K, et al. Iron leakage owing to blood–brain barrier disruption in small vessel disease CADASIL. *Neurology*. 2020;95:e1188.
- Walsh J, Tozer DJ, Sari H, et al. Microglial activation and blood–brain barrier permeability in cerebral small vessel disease. *Brain*. 2021;144:1361–1371.
- Zhao Z, Nelson AR, Betsholtz C, Zlokovic BV. Establishment and dysfunction of the blood–brain barrier. *Cell*. 2015;163:1064–1078.
- Dickie BR, Parker GJM, Parkes LM. Measuring water exchange across the blood–brain barrier using MRI. *Prog Nucl Magn Reson Spectrosc*. 2020;116:19–39.
- Raja R, Rosenberg GA, Caprihan A. MRI measurements of blood–brain barrier function in dementia: A review of recent studies. *Neuropharmacology*. 2018;134:259–271.
- St Lawrence KS, Owen D, Wang DJJ. A two-stage approach for measuring vascular water exchange and arterial transit time by diffusion-weighted perfusion MRI. *Magn Reson Med*. 2012;67: 1275–1284.
- Wang J, Fernández-Seara MA, Wang S, St Lawrence KS. When perfusion meets diffusion: *In vivo* measurement of water permeability in human brain. *J Cereb Blood Flow Metab*. 2007;27: 839–849.
- Shao X, Ma SJ, Casey M, D'Orazio L, Ringman JM, Wang DJJ. Mapping water exchange across the blood–brain barrier using 3D diffusion-prepared arterial spin labeled perfusion MRI. *Magn Reson Med*. 2019;81:3065–3079.
- Gold BT, Shao X, Sudduth TL, et al. Water exchange rate across the blood–brain barrier is associated with CSF amyloid- $\beta$  42 in healthy older adults. *Alzheimers Dement*. 2021;17:2020–2029.
- Shao X, Jann K, Ma SJ, et al. Comparison between blood–brain barrier water exchange rate and permeability to gadolinium-based contrast agent in an elderly cohort. *Front Neurosci*. 2020; 14:571480.
- Uchida Y, Kan H, Sakurai K, et al. APOE  $\epsilon$ 4 dose associates with increased brain iron and  $\beta$ -amyloid via blood–brain barrier dysfunction. *J Neurol Neurosurg Psychiatry*. Published online 28 April 2022. doi: 10.1136/jnnp-2021-328519
- Ohene Y, Harrison IF, Nahavandi P, et al. Non-invasive MRI of brain clearance pathways using multiple echo time arterial spin labeling: An aquaporin-4 study. *Neuroimage*. 2019;188:515–523.
- Ibata K, Takimoto S, Morisaku T, Miyawaki A, Yasui M. Analysis of aquaporin-mediated diffusional water permeability by coherent anti-stokes Raman scattering microscopy. *Biophys J*. 2011;101:2277–2283.
- MacAulay N, Zeuthen T. Water transport between CNS compartments: Contributions of aquaporins and cotransporters. *Neuroscience*. 2010;168:941–956.
- Verdura E, Hervé D, Scharrer E, et al. Heterozygous *HTRA1* mutations are associated with autosomal dominant cerebral small vessel disease. *Brain*. 2015;138:2347–2358.



20. Lee Y-C, Chung C-P, Chao N-C, et al. Characterization of heterozygous HTRA1 mutations in Taiwanese patients with cerebral small vessel disease. *Stroke*. 2018;49:1593-1601.
21. Coste T, Hervé D, Neau JP, et al. Heterozygous HTRA1 nonsense or frameshift mutations are pathogenic. *Brain*. 2021;144:2616-2624.
22. Hamilton OKL, Backhouse EV, Janssen E, et al. Cognitive impairment in sporadic cerebral small vessel disease: A systematic review and meta-analysis. *Alzheimers Dement*. 2021;17:665-685.
23. Shao X, Wang Y, Moeller S, Wang DJJ. A constrained slice-dependent background suppression scheme for simultaneous multislice pseudo-continuous arterial spin labeling. *Magn Reson Med*. 2018;79:394-400.
24. Wardlaw JM, Smith EE, Biessels GJ, et al. Neuroimaging standards for research into small vessel disease and its contribution to ageing and neurodegeneration. *Lancet Neurol*. 2013;12:822-838.
25. Staals J, Makin SDJ, Doubal FN, Dennis MS, Wardlaw JM. Stroke subtype, vascular risk factors, and total MRI brain small-vessel disease burden. *Neurology*. 2014;83:1228-1234.
26. Shao X, Tisdall MD, Wang DJ, van der Kouwe AJW. Prospective motion correction for 3D GRASE pCASL with volumetric navigators. *Proc Int Soc Magn Reson Med Sci Meet Exhib Int Soc Magn Reson Med Sci Meet Exhib*. 2017;25:0680.
27. Das AS, Regenhardt RW, Vernooij MW, Blacker D, Charidimou A, Viswanathan A. Asymptomatic cerebral small vessel disease: Insights from population-based studies. *J Stroke*. 2019;21:121-138.
28. Uchida Y, Kan H, Sakurai K, et al. Magnetic susceptibility associates with dopaminergic deficits and cognition in Parkinson's disease. *Mov Disord*. 2020;35:1396-1405.
29. ter Telgte A, van Leijssen EMC, Wiegertjes K, Klijn CJM, Tuladhar AM, de Leeuw F-E. Cerebral small vessel disease: From a focal to a global perspective. *Nat Rev Neurol*. 2018;14:387-398.
30. Bang J, Spina S, Miller BL. Frontotemporal dementia. *Lancet*. 2015;386:1672-1682.
31. Yan L, Liu CY, Wong K-P, et al. Regional association of pCASL-MRI with FDG-PET and PiB-PET in people at risk for autosomal dominant Alzheimer's disease. *Neuroimage Clin*. 2018;17:751-760.
32. Nasreddine ZS, Phillips NA, Bédirian V, et al. The Montreal Cognitive Assessment, MoCA: A brief screening tool for mild cognitive impairment. *J Am Geriatr Soc*. 2005;53:695-699.
33. Palomares JA, Tummala S, Wang DJJ, et al. Water exchange across the blood–brain barrier in obstructive sleep apnea: An MRI diffusion-weighted pseudo-continuous arterial spin labeling study. *J Neuroimaging*. 2015;25:900-905.
34. Huang J, Li J, Feng C, et al. Blood–brain barrier damage as the starting point of leukoaraiosis caused by cerebral chronic hypoperfusion and its involved mechanisms: Effect of agrin and aquaporin-4. *Biomed Res Int*. 2018;2018:2321797.
35. Hase Y, Chen A, Bates LL, et al. Severe white matter astrocytopathy in CADASIL. *Brain Pathol*. 2018;28:832-843.
36. Haj-Yasein NN, Vindedal GF, Eilert-Olsen M, et al. Glial-conditional deletion of aquaporin-4 (*Aqp4*) reduces blood–brain water uptake and confers barrier function on perivascular astrocyte endfeet. *Proc Natl Acad Sci U S A*. 2011;108:17815-17820.
37. MacAulay N. Molecular mechanisms of brain water transport. *Nat Rev Neurosci*. 2021;22:326-344.
38. Xu Z, Xiao N, Chen Y, et al. Deletion of aquaporin-4 in APP/PS1 mice exacerbates brain  $\text{A}\beta$  accumulation and memory deficits. *Mol Neurodegener*. 2015;10:58.
39. Hainsworth AH, Oommen AT, Bridges LR. Endothelial cells and human cerebral small vessel disease: Endothelial cells and SVD. *Brain Pathology*. 2015;25:44-50.
40. Tikka S, Baumann M, Siitonen M, et al. CADASIL and CARASIL. *Brain Pathol*. 2014;24:525-544.
41. Armulik A, Genové G, Mäe M, et al. Pericytes regulate the blood–brain barrier. *Nature*. 2010;468:557-561.